A Fast and Accurate Iris Recognition Method Using the Complex Inversion Map and 2DPCA

Sepehr Attarchi[1], Karim Faez[2], Amin Asghari[3]
[1, 3] *Electrical Engineering Department, Amirkabir University of Technology, Tehran, Iran, {threepehr, a_asghari }@aut.ac.ir*
[2] *Professor of Electrical Engineering Department, Amirkabir University of Technology, Tehran, Iran, kfaez@aut.ac.ir*

Abstract

Iris recognition is one of the most reliable biometric technologies. In this paper, we presented a novel method for iris recognition, using a complex mapping procedure and best-fitting line for the iris segmentation and 1D Gabor filter with 2DPCA for the recognition approach. We used an intensity threshold method with Canny edge detector to extract the rough region of the pupil. For the outer boundary a median filter with prewitt compass edge detector were used to localize the rough region of the outer boundary. By selecting the bottom point of the pupil (which is not usually occluded by the eyelids and eyelashes) as a reference point, two sets of intersecting points between the horizontal lines and pupil's inner and outer boundaries were created. Each point set was map into a new complex domain using the complex inversion map function and the best-fitting line was found on the range. Exact inner and outer boundaries of the iris were found by remapping the best-fitting lines to original domain. In the recognition procedure, we used the real term of 1D Gabor filter. In order to reduce the dimensionality of the extracted features, the new introduced 2DPCA method was used. We tested our proposed algorithm by implementing a ground truth method. Experimental results show that the proposed method has an encouraging performance in both segmentation and recognition approaches.

1. Introduction

Biometric personal identification is one of the most interesting topics in recent years. By increasing demands for security in the societies, the old methods of personal identification are not reliable anymore. Iris recognition is the most accurate biometrics which has received increasing attention in departments which require high security. Iris segmentation is an important step in the iris recognition approaches. Iris is usually occluded by top and down eyelids and eyelashes, makes it difficult to extract the iris region accurately. Also reflection spots may cause some problems during the segmentation procedure. Most of the previous segmentation methods use an integrodifferential operator or Hough transform in order to localize the iris boundary accurately. Daugman [1-3] proposed an integrodifferential operator in order to detect the inner and outer boundary of the iris. Ma et al. [4] used an edge detection method and Hough transform for iris localization. Wildes [5] used Hough transform method and a voting procedure in order to locate the iris boundaries. Although these methods are all accurate and robust to noise, but due to their massive computations, speed of the segmentation in these methods is low and they usually take a lot of time in order to segment the iris boundaries. In the recent years, more studies were carried out to improve the speed of the iris segmentation. Xiaofu He [6] proposed a new segmentation method for hand-held capture devices. They used groups of 3 points and a geometric approach to find the pupil boundary. They used Hough transform to detect the outer boundary of the iris. Li Yu [7] used a new method for iris segmentation in their proposed method. They scanned the binarized iris image horizontally to find the longest chord in the image, assuming the point that the longest chord will be the diameter of the pupil. They calculated the outer boundary parameter using an edge detection method in certain regions.

In this paper, we proposed a new segmentation method using complex inversion map and best-fitting line on the range. We binarized the image using an

978-0-7695-3131-1/08 $25.00 © 2008 IEEE
DOI 10.1109/ICIS.2008.69

intensity threshold method. After this, the binarized image was denoised using a morphological operation (opening). In order to detect the boundary of the pupil, canny edge detector was applied to the denoised image. By finding the bottom point of the pupil, a set of intersecting points between the horizontal lines and the pupil boundary was created. By choosing a reference point in the set, all the points in the set were mapped into a new domain, using the complex inversion map. The best-fitting line was calculated in the new domain. By remapping the best-fitting line, the best-fitting circle for inner pupil boundary was found. For the outer boundary, a median filter was applied to the iris image to smooth the iris pattern as much as possible. Then we used a prewitt compass operator [8] in order to detect the outer boundary of the iris. We excluded the pupil region regarding the calculated pupil center and radius and the prior-knowledge that Iris radius has been typically between 90-125 pixels [9]. A set of intersecting points between the horizontal lines and the iris outer boundary was created and the same procedure, as used in pupil boundary detection, was performed to extract the exact region of the outer boundary. Upper part of the iris is usually occluded with top eyelid and eyelashes; therefore the lower part of the iris was used for the recognition approach. In this step, in order to reduce the processing time, we used the real term of a conventional 1D Gabor filter. For reducing the dimensionality of the extracted features, we used in new method called 2DPCA, which is based on 2D metrics as opposed to standard PCA, which is based on 1D vectors.

The rest of the paper is organized as follows: Section 2 introduces the pupil boundary detection. Section 3 presents outer boundary detection. Iris Normalization, Encoding and matching are presented in section 4. Experimental results are given in section 5; finally section 6 concludes this paper.

2. Pupil Boundary Detection

The iris is a thin circular part which lies between the pupil and sclera. Upper and the lower part of the iris are usually occluded by the top and down eyelids and eyelashes. Both the inner and the outer boundary of the iris can be approximately taken as a circle. We used an intensity threshold method to detect the boundary of the pupil considering the point that the pupil is usually darker than its surroundings.

2.1. Pupil Region Extraction

In order to extract the exact region of the pupil, an intensity threshold method was used. Since the pupil is usually darker than the other parts of the image, we binarized the image using a threshold. The threshold was selected using the gray level histogram of the iris image. Fig. 1(a) shows the original iris image and Fig. 1(b) shows iris image after applying the threshold.

Upper part of the pupil is usually occluded by top eyelid and eyelashes which their intensity is similar to pupil. On the contrary the lower part of pupil is rarely affected by any eyelids and eyelashes. In order to remove the noisy effect of eyelids and eyelashes in the binarized image, we used a morphological operation (opening). First we applied a disk operator to erode the image, and then the same disk was used to dilate the eroded image. Fig. 1(c) shows the result of applying the morphological operator. For extracting the rough pupil region in the iris image, we used a Canny edge detector to detect the edges of the pupil as shown in Fig 1. (d).

2.2. Radius and Center Calculation

As we mentioned before, bottom point of pupil is robust to noise and usually not occluded by the top and bottom eyelids and eyelashes. In addition, lower eyelid and eyelashes intensities are greater than pupil intensity [9]. Therefore they can be completely removed by applying the threshold. We scanned the image horizontally in order to locate the bottom point of the pupil. By finding the bottom point, we scanned the pupil horizontally from the bottom upward at regular intervals and created a set of intersecting points between the horizontal lines and pupil boundary. In the next step, a complex inversion map is used to estimate the best fitting circle of the pupil boundary. Complex inversion map is defined as:

$$f(z)=\frac{1}{z} \qquad (1).$$

$$z=x+iy$$

This function maps a circle on the domain which passes through the origin, to a straight line on the range. Regarding this, 5 steps are performed to get the best fitting circle for inner boundary:

1. Rearranging the point set by converting each pair (x, y) to a complex number $x+iy$.
2. Randomly selecting a reference point from the reshaped point set.

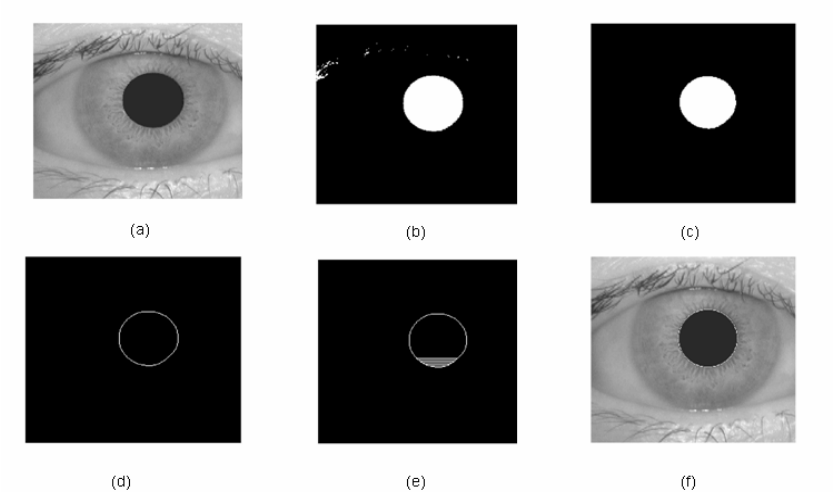

Fig. 1. Pupil localization. (a) Iris image. (b) Binarized image. (c) Denoised image after applying morphological operator. (d) Edge image. (e) Horizontal lines intersecting pupil boundary. (f) Detected pupil boundary.

3. Subtracting the coordinates of the reference point from the other points in the set.
4. Mapping each point in the point set using the complex inversion map. x and y in the new domain are calculated from the equations below:

$$u = \frac{x}{x^2 + y^2} \qquad (2).$$
$$v = \frac{-y}{x^2 + y^2}$$

5. Finding the best fitting straight line through the mapped points in the new domain. With the prior-knowledge that the vertical offsets from a line are almost always minimized instead of the perpendicular offset, the best fitting line with the parametric equation;

$$f(x, y) = ax + b \qquad (3),$$

Which passes through n different points is calculated as below:

$$a = \frac{\sum_{i=1}^{n} y_i \sum_{i=1}^{n} x_i^2 - \sum_{i=1}^{n} x_i \sum_{i=1}^{n} x_i y_i}{n \sum_{i=1}^{n} x_i^2 - \left(\sum_{i=1}^{n} x_i^2\right)^2} \qquad (4).$$
$$b = \frac{n \sum_{i=1}^{n} y_i x_i - \sum_{i=1}^{n} x_i \sum_{i=1}^{n} y_i}{n \sum_{i=1}^{n} x_i^2 - \left(\sum_{i=1}^{n} x_i^2\right)^2}$$

6. Remapping the calculated equation to obtain the best fitting circle for pupil boundary.

Fig 1. (e) shows the horizontal lines which intersect the pupil boundary and Fig 1. (f) illustrates the extracted pupil boundary.

3. Outer Boundary Detection

Detecting the outer boundary of the iris is more complicated than the inner boundary because of the little contrast between the iris and the sclera. In order to detect the outer boundary, we used 6 major steps as mentioned below:

1. Applying a 13×13 median filter to the iris image, mainly to smooth or completely remove the iris pattern. Fig 2. (b) shows the filtered image.
2. Convolving the left side of the image by 0° oriented prewitt compass edge detector and the right side by 180° oriented prewitt compass edge detector to detect the outer boundary edges.
3. Using an intensity threshold method in order to exclude the weak detected edges. Result is shown in Fig 2. (c).
4. Excluding the pupil region as shown in Fig 2. (d), regarding the calculated pupil center and radius in the previous section and the prior-knowledge that Iris radius has typically been 90-125 pixels [9].
5. Scanning the image horizontally from the bottom of the pupil upward and downward at regular intervals and created a set of the intersecting points between the horizontal

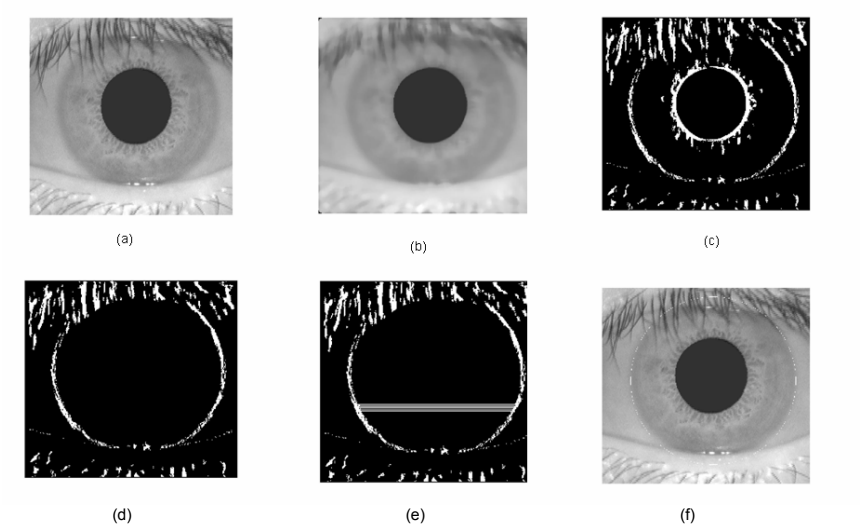

Fig. 2. Outer boundary detection. (a) Iris image. (b) Iris image after applying median filter. (c) Iris image after applying Prewitt compass edge detector. (d) Edge image after excluding the pupil boundary. (e) Horizontal lines intersecting iris outer boundary. (f) Detected iris outer boundary.

lines and outer iris boundary. Fig 2. (e) shows the horizontal lines which intersect the outer iris boundary

6. Performing all the steps mentioned in section 2.2 to find the exact outer boundary of the iris.

4. Normalization, Encoding and Matching

Different people have different iris sizes. Even the size of the iris captured from one person may be different due to illumination variations. In order to solve this problem we used daugman's rubber sheet model to unwrap the iris into the rectangular block of the fixed size 12×240. Upper part of the iris pattern is usually occluded by the top eyelid and eyelashes. In order to avoid these noisy effects in the extracted iris pattern, we used only the lower half of the iris. Therefore we excluded the first 120 columns of the normalized iris images making our extracted template of the size 12×120. Generally, Gabor filters contain both real and imaginary terms. We used the real term of a conventional 1D Gabor filter as shown below:

$$G(x) = A.e^{-\pi\left(\frac{(x-x_0)^2}{\sigma^2}\right)}\cos\left(2\pi u_0\left(x-x_0\right)\right) \quad (6)$$

Where A and σ and u_0 are the amplitude of the Gabor filter, kernel size and the frequency of the Gabor filter respectively. Considering the point that the 2DPCA is essentially working on the rows of the image [10], the 2DPCA was used in order to reduce the dimensionality of the extracted features. After applying the 1D Gabor filter to each row of normalized iris image, we constructed a covariance matrix using the extracted 2D features. Assuming the training set of the extracted features to be $F_1, F_{2,}..., F_k$, each of which is of size 12×120. The average of the set is defined as:

$$\overline{F} = \frac{1}{k}\sum_{i=1}^{k} F_i \quad (7).$$

Then the covariance matrix is given by:

$$Cov = \frac{1}{k}\sum (F_i - \overline{F})^T (F_i - \overline{F}) \quad (8),$$

which is 120×120 matrix. After calculating the eigenvalues and eigenvectors of the covariance matrix, we chose the *m* eigenvectors corresponding the *m* highest eigenvalues (X_m) and calculated the new low dimensional 2D features (Y_m) as:

$$Y_k = F.X_k (k = 1,2,..., m) \quad (9).$$

At the final step, we used the nearest neighbor classifier for the purpose of classification.

5. Experimental Results

In order to evaluate the effectiveness of our roposed algorithm, extensive experiments were performed. We designed and implemented a semi-manual graound

Table 1: Comparison results of the inner and the outer parameter

Methods	Pupil center distance (pixels)		Pupil Radius distance (pixels)		Accuracy (%)	
	Mean	Standard Deviation	Mean	Standard Deviation	Center	Radius
Proposed	1.24	1.14	1.12	1.02	99.86	99.95
Xiaofu He method	2.20	1.43	1.44	1.24	99.33	99.92
	Outer boundary center distance (pixels)		Outer boundary radius distance (pixels)		Accuracy (%)	
Proposed	3.26	2.63	1.34	1.87	98.78	99.55
Xiaofu He method	4.2009	3.7525	1.3858	2.9076	98.0	99.42

truth method as Xiaofu He et. al. used in [6] to evaluate the accuracy of our proposed segmentation method. Further we tested our iris recognition approach in both identification and verification mode. We used the public database CASIA [11] which includes 756 iris images from 108 different people. Each person has 7 different iris images captured in 2 sessions with 320×280 pixels in 256 gray levels.

5.1. Segmentation Results

We tested our proposed segmentation method by implementing a semi-manual ground truth method similar to what Xiaofu He et.al. used during their experiments [6]. We used the same idea to evaluate the performance of our segmentation results with a little change due to differences between our proposed method and theirs. Following steps were performed in order to generate the ground truth:

1. Extracting the pupil region using the same method in section 2.1.
2. Detecting the edge of the pupil as described in section 2.1, also deleting the noises in the image manually.
3. Calculating the pupil center and radius using Hough transform.
4. Detecting the edge of the outer boundary of the iris using the method described in section 3.
5. Excluding the pupil region and deleting the noises in the image manually.
6. Calculating the outer boundary circle parameter using the Hough transform.

After performing the ground truth method, we compared the result of the segmentation obtained by this method with our proposed method. We calculated the distance between the center and radius of the inner and outer boundary circles in both ground truth and our proposed method, considering the point that the smaller distance results in a better segmentation. If the distance between our proposed method and the ground truth method for pupil center and radius was within the 8 pixels, we considered this as a success. Otherwise the result is considered as a failure. For the outer boundary the distance threshold was selected 15 pixels as used by Xiaofu He in [6]. Table 1 shows the segmentation results of the inner and the outer boundary. Also the Xiaofu He et. al. results were mentioned in the table. As it is clear, our algorithm has better segmentation results in accuracy of segmentation. All the calculation was implemented using Matlab 7 on an Intel Pentium IV 2.66G processor with 512 MB memory, whereas Xiaofu He et. al. implemented their proposed method using Matlab 7 on an Intel Pentium IV 3G processor with 512 MB memory. The execution time for inner boundary detection was 0.08s and 0.055s for outer boundary detection. Whereas for the Xiaofu He the execution times were 0.18s and 0.56s for the inner and outer boundary detection respectively.

5.2. Recognition Results

Proposed recognition method was tested in both identification and verification modes. As mentioned before, the lower part of the iris was used to create an iris template. We used the real term of a conventional 1D Gabor filter as shown in Eq. (6), with $\sigma = 20$ and $u_0 = 0.055$. Also we set the sum of all the coefficients of the Gabor filter to 0 for the normalization of the filtering coefficient. For the reduction of extracted features dimensionality, the new introduced 2DPCA was used. We found the best performance of our proposed algorithm by setting the number of eigenvectors, *m*, to 16, making our features dimensionality to 12×16 2D matrices. In identification mode, our algorithm reached the correct recognition rate of 99.32% at *m*=16 using the nearest neighbor method as the classifier. The first 4 iris images of each person (session 1 in CASIA

database and the first image in session 2) were chosen to build a template and other iris images for testing. Table 2 shows the recognition rate achieved with different number of training images for each person in CASIA database. The small iris template dimensionality and high identification rate of our proposed algorithm shows effectiveness of our algorithm in identification mode. Also we used the ROC curve to evaluate the performance of our algorithm in verification mode. The ROC curve is false acceptance rate versus false rejection rate. The minimum error occurs when the FAR and FRR are equal, where we reached the minimum error rate of 0.68%.

6. Conclusion

In this paper, we proposed a new iris recognition method using the complex inversion map and the best-fitting line for the iris segmentation and conventional 1D Gabor filter with 2DPCA for the recognition approach. We extracted the pupil region using an intensity threshold method and then the binarized image was denoised using a morphological operation. Canny edge detector was used to detect the edge of the pupil boundary. By finding the bottom point of the pupil, a set of intersecting points between the horizontal lines and the pupil boundary was created. After choosing a reference point from the set, all the points in the set were mapped on the range using the complex inversion map. Best fitting line was calculated in the new domain and by remapping the line, the best fitting circle for inner pupil boundary was found. For the outer boundary, first we used a median filter to smooth the iris pattern as much as possible. Then we used a prewitt compass operator in order to detect the outer boundary of the iris. The same mapping procedure was performed to extract the exact region of the outer boundary. We implemented a ground truth method in order to evaluate the accuracy of our proposed segmentation algorithm. We reached the correct segmentation rate of 99.86, 99.95, 98.78 and 99.55 for the pupil center, pupil radius, outer boundary circle center and outer boundary radius respectively. The average execution time for inner boundary detection was 0.08s and 0.055s for outer boundary detection using Matlab 7 on an Intel Pentium IV 2.66G processor with 512 MB memory. Further we calculated the recognition results. We used the real term of a 1D Gabor filter to extract the iris details.

Table 2: Recognition rate of the proposed algorithm for different number of training images

Number of training images	1	2	3	4
Recognition rate (%)	88.6	90.1	94.55	99.32

In order to reduce the dimensionality of the extracted features, we applied the new introduced 2DPCA method. Also we used the nearest neighbor classifier for the purpose of classification. Our algorithm reached the correct recognition rate of 99.32%.

Acknowledgement

This research is supported by Iranian telecommunication research center (ITRC).

References

[1] J.G. Daugman, "High confidence visual recognition of person by a test of statistical independence", IEEE Trans. Pattern Anal. Mach. Intell. 15 (11) (1993) 1148-1160.

[2] J.G. Daugman, "The importance of being random: statistical principles of iris recognition", Pattern Recognition 36 (2) (2003) 279-291.

[3] J.G. Daugman, "How iris recognition works", IEEE Trans. Circuits Syst. Video Technol. 14 (1) (2004) 21-30.

[4] J. Huang, Y. Wang, T. Tan et al., "A new iris segmentation method for recognition", Proceedings of the 7th International Conference on Pattern Recognition, vol.3, 2004, pp. 554-557.

[5] R. Wildes, "Iris recognition: an emerging biometric technology", Proc. IEEE 85 (9) (1997) 1348-1363.

[6] Xiaofu He, Pengfei Shi, "A New segmentation approach for iris recognition based on hand-held capture device", Pattern Recognition 40 (2007) 1326-1333.

[7] Li Yu, David Zhang, Kuanquan Wang, "The relative distance of key point based iris recognition", Pattern Recognition 40 (2007) 423-430.

[8] www.cee.hw.ac.uk/hipr/html/prewitt.html

[9] R. T. Al-Zubi, D.I. Abu-Al_nadi, "Automated personal identification system based on human iris analysis", Pattern Anal Applic (2007) 10:147-164.

[10] Daoqiang Zhang, Zhi-Hua Zhou, "$(2D)^2$PCA: 2-Directional 2-Dimensional PCA for Efficient Face Representation and Recognition", Nanjing University of Aeronautics and Astronautics, Nanjing 210016, China.

[11] CASIA (2003) CASIA iris image database, http://www.sino-biometerics.com.